Nanoscale Advances

ROYAL SOCIETY OF CHEMISTRY

COMMUNICATION

View Article Online
View Journal | View Issue

Cite this: *Nanoscale Adv.*, 2020, **2**, 2293

Received 3rd March 2020
Accepted 27th April 2020

DOI: 10.1039/d0na00179a

rsc.li/nanoscale-advances

Small molecule-decorated gold nanoparticles for preparing antibiofilm fabrics†

Le Wang,‡[ab] Michal Natan,‡[c] Wenshu Zheng,[b] Wenfu Zheng,*[bd] Shaoqin Liu,*[a] Gila Jacobi,[c] Ilana Perelshtein,[e] Aharon Gedanken,[e] Ehud Banin*[c] and Xingyu Jiang*[bf]

The increase in antibiotic resistance reported worldwide poses an immediate threat to human health and highlights the need to find novel approaches to inhibit bacterial growth. In this study, we present a series of gold nanoparticles (Au NPs) capped by different N-heterocyclic molecules (N_Au NPs) which can serve as broad-spectrum antibacterial agents. Neither the Au NPs nor N-heterocyclic molecules were toxic to mammalian cells. These N_Au NPs can attach to the surface of bacteria and destroy the bacterial cell wall to induce cell death. Sonochemistry was used to coat Au NPs on the surface of fabrics, which showed superb antimicrobial activity against multi-drug resistant (MDR) bacteria as well as excellent efficacy in inhibiting bacterial biofilms produced by MDR bacteria. Our study provides a novel strategy for preventing the formation of MDR bacterial biofilms in a straightforward, low-cost, and efficient way, which holds promise for broad clinical applications.

1 Introduction

The increasing resistance of bacteria to antibiotic therapy is a growing concern for doctors and poses a public health threat worldwide. In the last two decades, due to the continuous consumption of antibiotics, multidrug-resistant (MDR) bacteria that cause serious infections have emerged.[1] These bacteria exhibit resistance to almost all commercially available antibiotics, increasing the morbidity and mortality of patients as well as medical costs.[2] An additional strategy utilized by bacteria to increase antimicrobial resistance is the formation of biofilms. Biofilms, which are structured communities of bacteria, can form on abiotic and biotic surfaces and are inherently more resistant to antibiotics than planktonic bacteria. Further, biofilms contribute to most device-related infections since they have the capability to evade the immune system and are very difficult to eradicate.[3–5] At present, the methods for prevention and treatment of bacterial biofilms mainly include physical clearance, chemical removal and biological clearance, such as with ultrasound, amphiphilic cationic molecules, metal ions, surfactants, enzymes, peptides, and monoclonal antibodies. As the development of novel antibiotics has been limited, there is an urgent need to find novel approaches to combat antibacterial resistance. The large surface area of nanoparticles (NPs) provides a high number of functional sites and offers opportunities for the discovery of novel compounds with antimicrobial activity.[6] Various types of NPs, such as silver (Ag),[7] metal oxides like zinc oxide (ZnO)[8–10] and copper oxide (CuO),[11,12] carbon nanotubes,[13] and graphene,[14] have received great attention due to their potential antimicrobial activities. Although these NPs show promising results, they have varying degrees of toxicity.[15,16] Compared to other NPs, gold NPs (Au NPs) have many merits, including controllable synthesis, easy surface modification, and excellent biocompatibility,[17–19] making them ideal agents for potential clinical applications. During the past few years, we have developed a series of small molecule-activated antibacterial Au NPs that are effective against MDR bacteria.[17–19] Au NPs themselves generally have no antimicrobial activity, but when modified with functional groups, such as mercaptan, amine, hydrosulphonyl, or phosphonic compounds, these small molecule-capped Au NPs show effective antibacterial activities.[20,21]

[a]*School of Life Science and Technology, Harbin Institute of Technology, 2 Yikuang Road, Nangang District, Harbin 150001, P. R. China. E-mail: shaoqinliu@hit.edu.cn*
[b]*Beijing Engineering Research Center for BioNanotechnology, CAS Key Laboratory for Biological Effects of Nanomaterials and Nanosafety, National Center for NanoScience and Technology, Beijing 100190, P. R. China. E-mail: zhengwf@nanoctr.cn*
[c]*The Institute for Advanced Materials and Nanotechnology, The Mina and Everard Goodman Faculty of Life Sciences, Bar-Ilan University, Ramat-Gan 52900, Israel. E-mail: ehud.banin@biu.ac.il*
[d]*GBA Research Innovation Institute for Nanotechnology, Guangdong 510700, P. R.China*
[e]*The Institute for Advanced Materials and Nanotechnology, Department of Chemistry, Bar-Ilan University, Ramat Gan 5290002, Israel*
[f]*Department of Biomedical Engineering, Southern University of Science and Technology, No. 1088 Xueyuan Rd, Nanshan District, Shenzhen, Guangdong 518055, P. R. China. E-mail: jiang@sustech.edu.cn*

† Electronic supplementary information (ESI) available. See DOI: 10.1039/d0na00179a

‡ These authors contributed to this work equally.

NPs could also be modified and embedded in or coated on various surfaces to provide them with unique properties. The ultrasound-assisted coating method is a convenient method for coating active NPs on substrates such as polymers,[22] metals,[23] and textiles.[24] By a one-step process, NPs can be synthesized and coated on the surface.[25,26] It was previously shown that sonochemically coated surfaces were highly durable and could withstand extensive washing cycles.[27] Taking into account the advantages of the ultrasound-assisted coating method, in the current work, we used ultrasound to coat fabrics with pre-prepared Au NPs. The coating mode was the "throwing stones" method, namely, the Au NPs were deposited on the surface by ultrasound waves. The approach was previously used for coating Al_2O_3 and MgO on textiles.[28]

In this study, we synthesized an array of N-heterocyclic molecule-coated gold NPs (N_Au NPs) by a one-pot synthesis approach (Fig. 1A). All these N-heterocyclic molecules have a –SH group, which serves as a protective agent for the synthesis of well-dispersed Au NPs. Among these N-heterocyclic molecules, 2-mercaptoimidazole (MI)- and 3-amino-1,2,4-triazole-5-thiol (ATT)-capped Au NPs have broad-spectrum antibiofilm effects. The N_Au NPs were potent antimicrobials targeting MDR bacteria, including methicillin-resistant *Staphylococcus aureus* (MRSA) and MDR *Escherichia coli* (MDR *E. coli*) *in vitro*. The N_Au NPs can directly come into contact with and disrupt the bacterial cell wall. Due to the unique antibacterial mechanism, the N_Au NPs may be less prone to inducing resistance among bacteria than antibiotics. In addition, we used ultrasound-assisted coating technology to fabricate antibiofilm fabrics, which can prevent the formation of biofilms for addressing the issue of MDR bacterial infections (Fig. 1B and C).

2 Experimental section

2.1 Materials

Sodium borohydride ($NaBH_4$), tetrachloroauric acid ($HAuCl_4 \cdot 3H_2O$), 2-mercaptoimidazole (MI, $M_w = 100.142$, CAS no. 872-35-5, soluble in methanol, $LD_{50,intraperitoneal}$, 200 mg kg^{-1}), 3-amino-1,2,4-triazole-5-thiol (ATT, $M_w = 116.145$, CAS no. 16691-43-3, soluble in water, pharmaceutical and pesticide intermediate), 6-amino-2-mercaptobenzothiazole (AMBT, $M_w = 182.266$, CAS no. 7442-07-1, $LD_{50,intraperitoneal}$, 150 mg kg^{-1}), 2-amino-6-mercaptopurine (AMP, $M_w = 167.192$, CAS no. 154-42-7, soluble in water, antitumor drug, $LD_{50,intraperitoneal}$, 54 mg kg^{-1}) and 6-aminopenicillanic acid (APA, $M_w = 216.258$, CAS no. 551-16-6, slightly soluble in water, $LD_{50,intraperitoneal}$, 1000 mg kg^{-1}) were obtained from Sigma (USA). All other chemicals and solvents were of reagent grade.

2.2 Preparation and characterization of N_Au NPs

In our previous work,[20] N_Au NPs were synthesized in methanol and may leave residual solvents in the final products, which may be harmful to mammalian cells and limit their applications. Thus, we did not carry out further experiments using these nanoparticles. In this study, different from the previous work, N_Au NPs were synthesized under aqueous conditions to safeguard their biocompatibility. N_Au NPs were prepared with

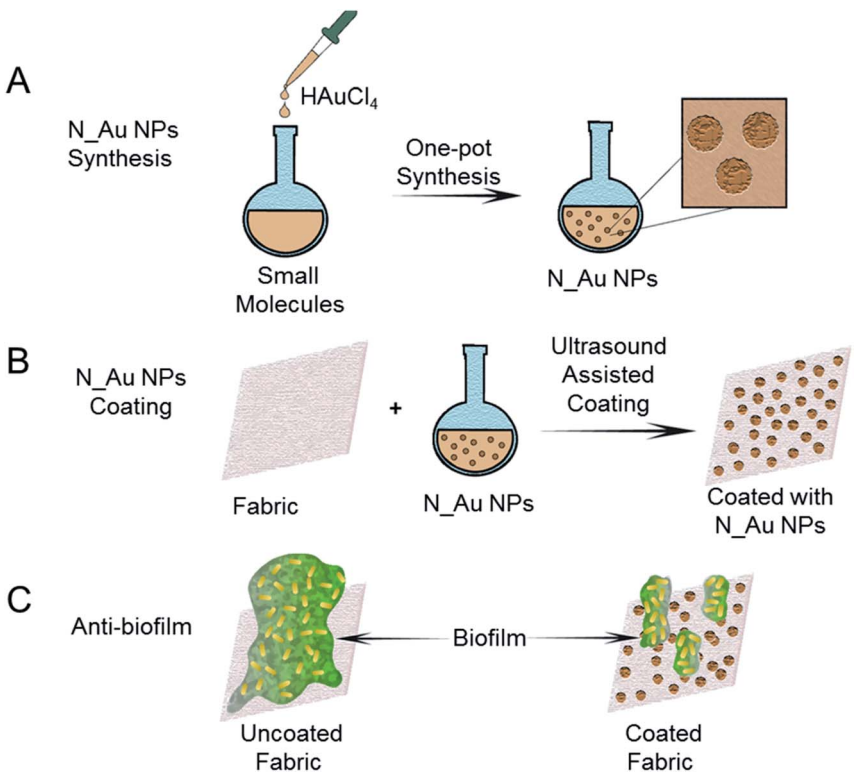

Fig. 1 Schematic illustration of the preparation process of antibiofilm fabrics coated with the N_Au NPs.

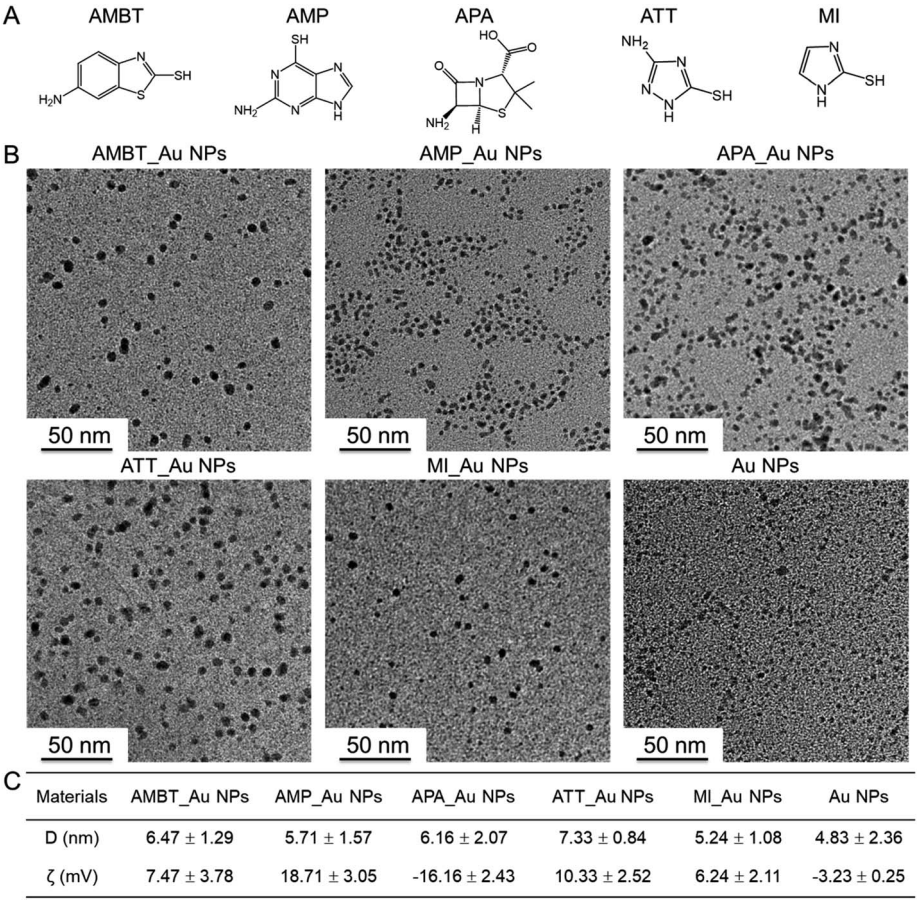

C

Materials	AMBT_Au NPs	AMP_Au NPs	APA_Au NPs	ATT_Au NPs	MI_Au NPs	Au NPs
D (nm)	6.47 ± 1.29	5.71 ± 1.57	6.16 ± 2.07	7.33 ± 0.84	5.24 ± 1.08	4.83 ± 2.36
ζ (mV)	7.47 ± 3.78	18.71 ± 3.05	-16.16 ± 2.43	10.33 ± 2.52	6.24 ± 2.11	-3.23 ± 0.25

Fig. 2 The morphology, size, dispersity, and zeta potential of the N_Au NPs. (A) The structure of N-heterocyclic molecules. (B) TEM images of the Au NPs. (C) DLS analysis results of the N_Au NPs.

Table 1 MBC of N_Au NPs and Au NPs (μg ml^{-1}). The N_Au NP concentration was measured using the gold concentration through ICP and the concentration of small molecules was calculated *via* dividing their weights by the volume of their solutions

	Gram-negative bacteria		Gram-positive bacteria	
	E. coli	MDR *E. coli*	*S. aureus*	MRSA
AMBT	>128	>128	>128	>128
AMBT_Au NPs	16	16	16	32
AMP	>128	>128	>128	>128
AMP_Au NPs	16	16	32	32
APA	>128	>128	>128	>128
APA_Au NPs	7.5	15	>128	>128
ATT	>128	>128	>128	>128
ATT_Au NPs	8	8	32	32
MI	>128	>128	>128	>128
MI_Au NPs	8	8	16	16
Au NPs	>128	>128	>128	>128

a one-pot synthesis approach using the mechanism of reduction of $HAuCl_4 \cdot 3H_2O$ by $NaBH_4$. 0.1 mmol heterocyclic small molecules, 50 μl of triethylamine and 40 mg of Tween 80 were dissolved in 10 ml double-distilled water which was further mixed with 0.1 mmol of $HAuCl_4 \cdot 3H_2O$ and was stirred for 10 min in an ice-water bath. $NaBH_4$ (6 mg dissolved in 2 ml double-distilled water) was added dropwise with vigorous stirring and was kept undisturbed for an additional 2 h. The synthesis of the bare gold nanoparticles was similar, except we did not add the small molecules. After the reaction, the resulting solution was dialyzed with a dialysis bag (14 kDa MW cut-off, Solarbio) to remove the unreacted chemicals for 24 h and filtered through a 0.22 μm filter (Millipore). We characterized the morphologies of N_Au NPs by transmission electron microscopy (TEM, Tecnai G2 20 S-TWIN, FEI Company, USA) and determined the concentrations by measuring elemental gold with inductively coupled plasma analysis (ICP, iCAP 6300, Thermo Scientific, USA). We characterized the size and zeta potential of the samples by dynamic light scattering (DLS) on a Zetasizer Nano ZS (Malvern Company, England). We used the CONTIN method to obtain the size distribution and zeta potential of the NPs.

2.3 Sonochemical coating

Various dispersions containing the N_Au NPs were used for the sonochemical coating. A piece of fabric (4 × 4 cm) was

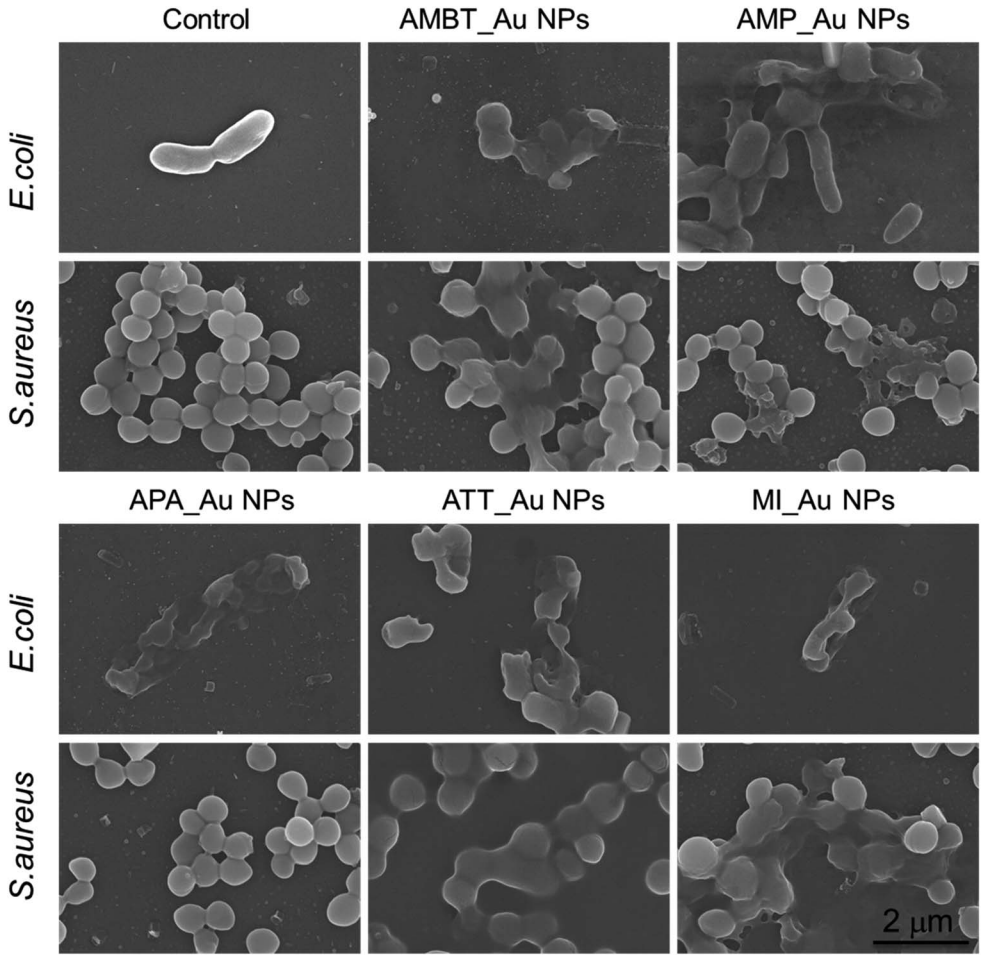

Fig. 3 Morphology of *E. coli* and *S. aureus* with and without N_Au NP treatment. Bacteria treated with phosphate buffered saline served as a negative control. Scale bar is 2 μm.

immersed in the solutions (20 ml) which were irradiated using an ultrasonic horn (Ti horn, with 30% booster efficiency, 750 W) for 30 min. After 10 min, the sonication beaker was placed in a cooling bath with a temperature of 40 °C during sonication. After the sonication, the fabric was washed with ethanol and dried at room temperature. The color of the fabric gradually changed from white to black, depending on the amount of the coated compound. The fabrics coated with different N_Au NPs were examined by high-resolution scanning electron microscopy (HR-SEM, Magellan, FEI microscope) at an accelerating voltage within the range of 5–15 kV. To improve the quality of the images, the samples were coated with a carbon layer by sputtering in a rarefied atmosphere of argon at 0.1–0.2 mbar by means of an Emitech K550 Sputter Coater. The amount of coating was determined by ICP analysis. A piece of coated fabric was immersed in 5 M HNO_3 and heated for 15 min. We added water in the solution which was boiled for another 15 min. The total volume of the solution was adjusted to 50 ml and measured by ICP for calculation of the gold ions.

2.4 Minimum bactericidal concentration (MBC) assay

Gram-negative bacteria (*e.g.*, *Escherichia coli*) can cause infection of the urinary tract, gastrointestinal tract and lungs, while Gram-positive bacteria (*e.g.*, *Staphylococcus aureus*) can cause infection of the skin and cartilage tissues. We chose Gram-negative *Escherichia coli* ATCC 25922 (*E. coli*) and Gram-positive *Staphylococcus aureus* ATCC 29213 (*S. aureus*), along with their MDR counterparts (*Klebsiella pneumoniae* ATCC® BAA-1898™ (MDR *K. pneumoniae*), *E. coli* ATCC® BAA-2452™ (MDR *E. coli*), and methicillin-resistant *S. aureus* ATCC 43300 (MRSA)) as model bacteria. All bacteria were cultured overnight at 37 °C under stirring (250 rpm) in Mueller Hinton growth medium (MH, BD Difco™, USA).

The antibacterial activity of the N_Au NPs was evaluated by measuring the MBC values. The overnight cultured bacteria were rinsed with phosphate buffered saline (PBS, Solarbio), re-suspended to the final bacterial concentration (10^5 colony-forming units (CFU) ml^{-1}) and treated with different concentrations of N_Au NPs in a 96-well plate (Greiner Bio-one) at 37 °C. After this, 10-fold serial dilutions (100 μl) were conducted, and the bacteria were plated on LB agar plates and incubated at 37 °C for 24 h. The growth of bacteria was monitored and quantified by viable cell counting and expressed as colony-forming units.

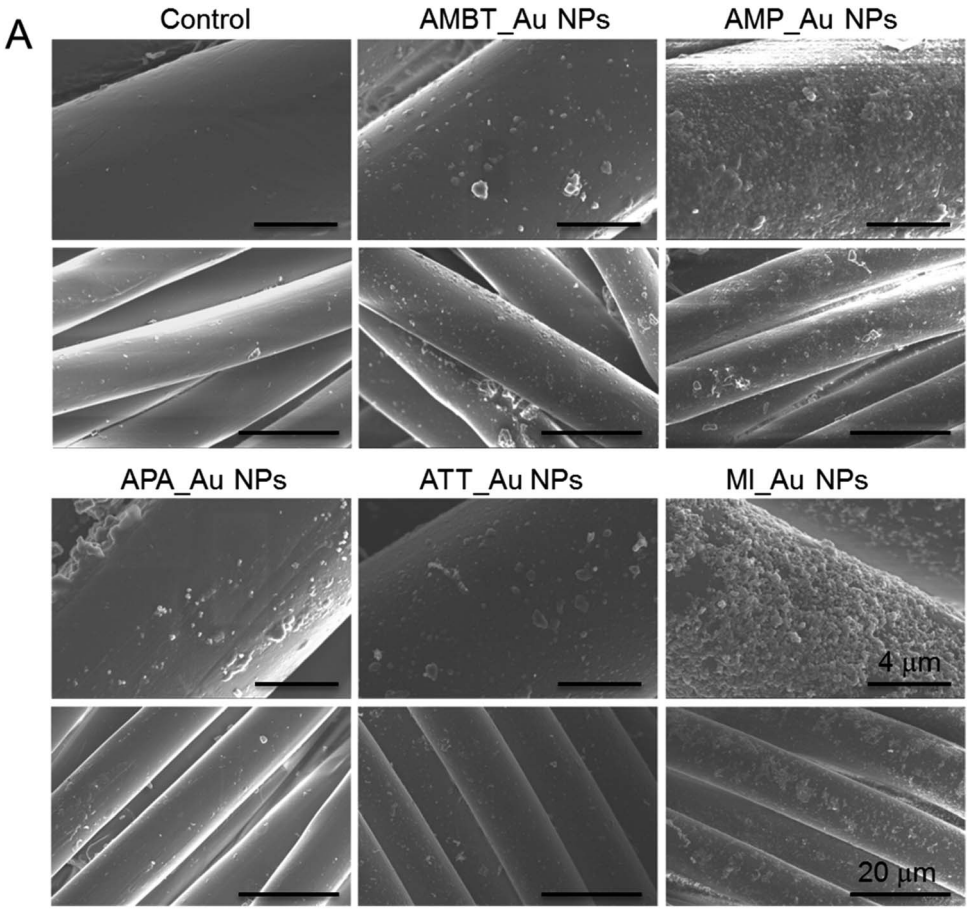

B

Materials	Control	AMBT_Au NPs	AMP_Au NPs
within the coated material (wt%)	/	0.0048	0.15
Materials	APA_Au NPs	ATT_Au NPs	MI_Au NPs
within the coated material (wt%)	0.0085	0.0012	0.015

Fig. 4 Characterization of the control fabrics and N_Au NP-coated fabrics. (A) SEM images of control fabrics or fabrics coated with different ligands. The scale bar was 4 μm or 20 μm. (B) ICP analysis of the coated fabrics showing the concentration of N_Au NPs within the different surfaces. The standard deviation of the ICP results corresponded to 1%.

2.5 Morphology changes of bacteria treated with N_Au NPs

Further, we verified the antibacterial mechanism of N_Au NPs by observing changes in the bacterial morphology. We fixed the N_Au NP-treated bacterial samples, *E. coli* ATCC 11775 (16 μg ml^{-1}) and *S. aureus* ATCC 29213 (32 μg ml^{-1}), for 4 h with 2.5% glutaraldehyde and ethanol dehydration (30%, 50%, 70%, 80%, 90%, 95%, and 100% (v/v, in water)) in sequence for SEM characterization. Bacteria treated with PBS were used as a negative control.

2.6 Antibacterial activity of N_Au NP-coated fabrics

Bacteria grown overnight were diluted in 1% MH to obtain a working solution with 10^5 colony-forming units (CFU) ml^{-1}. A 1 ml stock solution of the bacteria was transferred into a 24-well plate (DE-GROOT). The different fabrics (squares of 1 cm × 1 cm) were added to the well. The plates were then incubated at 37 °C for 20 h. Afterwards, 200 μl of the solution were transferred to the first row of a 96-well plate (Greiner Bio-One), and the other rows were filled with 180 μl of MH. Serial dilutions were conducted and the bacteria were spotted onto LB agar plates and incubated at 37 °C for 20 h. The growth of bacteria was quantified by counting viable cells.

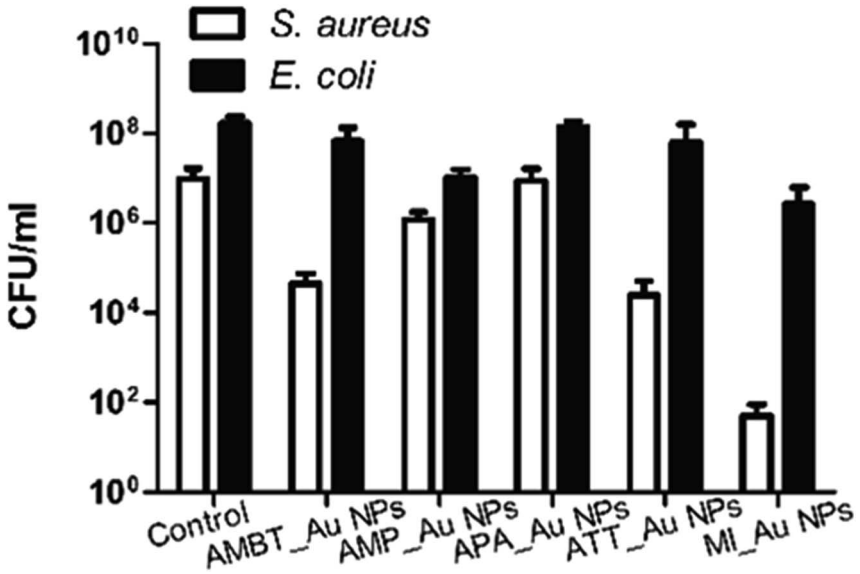

Fig. 5 Antibiofilm activity of N_Au NPs. Fabrics coated with either one of the N_Au NP materials were exposed to *E. coli* or *S. aureus* as described in the methods section, and the biofilm growth was determined using viable counts. The data represented the average of three independent experiments.

Table 2 Antibacterial activity of ATT_Au NP and MI_Au NP coated fabrics represented as log reduction in CFU

Bacteria	ATT_Au NPs	MI_Au NPs
S. aureus	2.4	5.2
E. coli	0.4	1.9
MRSA	3.5	4.1
MDR *E. coli*	0.2	1
MDR *K. pneumoniae*	0.2	1.3

2.7 Antibiofilm activity of N_Au NP-coated fabrics

The antibiofilm activity of the fabrics was determined by the static biofilm formation assay. Bacteria were grown overnight in MH growth medium. The bacteria were diluted in 1% MH to obtain a working solution with an OD_{595} of 0.3 for all bacterial strains besides *S. aureus* for which an OD_{595} of 0.01 was used. 1 ml of the stock solution of the bacteria was transferred into each well in a 24-well plate. The fabrics (square of 1 cm × 1 cm) were added into the wells. The plates were incubated for 20 h at 37 °C. The fabrics were rinsed twice with distilled water to remove the planktonic cells. The attached cells were scraped from the fabrics using 250 μl of 1% MH and a cell scraper (Greiner Bio-one). After scraping the cells, 200 μl of the 250 μl solution was transferred into a 96-well plate. The other wells were filled with 180 μl of MH. Serial dilutions were conducted, and the bacteria were spotted onto LB agar plates and incubated at 37 °C for 20 h. The growth of bacteria was determined by counting the viable cells.

2.8 Biological safety

Considering the comprehensive properties, we chose ATT_Au NP- and MI_Au NP-coated fabrics for the subsequent toxicity experiments. The *in vitro* cytotoxicity of the ATT_Au NPs and MI_Au NPs was evaluated by measuring the viability and morphology of human umbilical vein endothelial cells (HUVECs) and human aortic fibroblasts (HAFs) under treatment with the NPs. The cells were cultured in Dulbecco's Modified Eagle's Medium (DMEM) containing 1% penicillin–streptomycin and 10% fetal bovine serum at 37 °C with 5% CO_2. ATT_Au NPs and MI_Au NPs were diluted in DMEM to different concentrations, and the cell suspension (10^5 cells per ml) was added into them. The morphology of the cells was observed using an inverted microscope (DMI 6000B, Leica, Germany). The cell viability treated with ATT_Au NPs and MI_Au NPs was measured with a cell counting kit (CCK, Dojindo, Japan), and the absorbance at 450 nm was characterized using a microplate reader (Tecan infinite M200). We calculated the cell viability index using the following equation:

$$\text{Cell viability} = (OD_{experiment} - OD_{blank})/(OD_{control} - OD_{blank}) \times 100\%,$$

where $OD_{experiment}$ is the absorbance of the cell suspension with the addition of NPs, OD_{blank} is the absorbance of DMEM, and $OD_{control}$ is the absorbance of the cell suspension as a positive control.

3 Results and discussion

3.1 Characterization of N_Au NPs

We prepared different N_Au NPs by utilizing different N-heterocyclic molecules (Fig. 2A) as protective agents during the synthesis process. TEM analysis of the samples showed good dispersity and similar size distributions of the N_Au NPs, which were spherically shaped (Fig. 2B). The diameter distribution of the synthesized N_Au NPs was evaluated by DLS

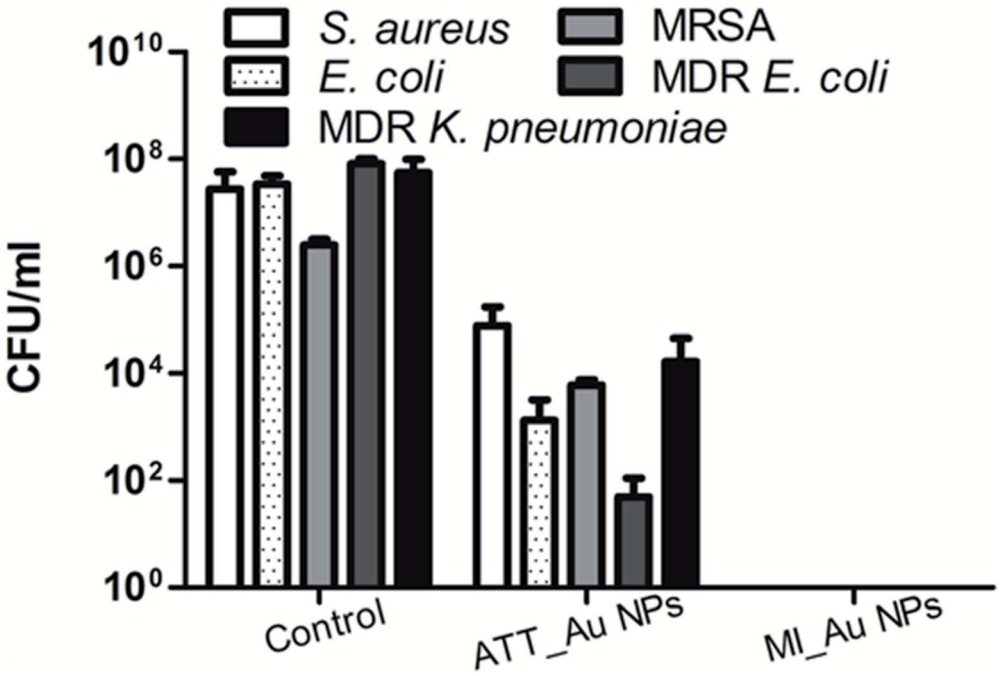

Fig. 6 Antibacterial activity of ATT_Au NP and MI_Au NP coated fabrics. Control designates uncoated fabrics. The results represent the average of three independent experiments.

(Fig. 2C and S1†). The diameter of Au NPs obtained by DLS was larger than the size obtained by TEM, which could be attributed to the hydration layer reflected by DLS. Due to the slight aggregation of the AMP_Au NPs and APA_Au NPs, the hydration radius was increased. Because DLS values can be affected by a number of factors, the DLS diameter alone cannot be used to accurately determine the size of the NPs. Thus, the small difference between the TEM diameter and DLS diameter is within the error of these experiments. The average diameter of the tested Au NPs was 6.47 nm (AMBT_Au NPs), 5.71 nm (AMP_Au NPs), 6.16 nm (APA_Au NPs), 7.33 nm (ATT_Au NPs), 5.24 nm (MI_Au NPs), and 4.83 nm (Au NPs), demonstrating their high stability and good dispersity (Fig. 2B). Zeta potential analysis indicated the successful functionalization of the N-heterocyclic molecules on the surface of the Au NPs (Fig. S2†). Gram-negative bacteria have a higher negative surface charge than Gram-positive bacteria.[29] All the N_Au NPs were positively charged except APA_Au NPs, which can interact strongly *via* electrostatic interactions with the Gram-negative bacteria and can facilitate the entrance of the NPs into bacteria. In contrast, the interactions of the NPs with Gram-positive bacteria with less negative charge will be less effective in initiating the break of the bacterial cell wall, which can significantly affect the antibacterial performance of N_Au NPs against Gram-positive bacteria (Fig. 2C).

3.2 Antibacterial activity of N_Au NPs

Initially, we evaluated the MBC of N_Au NPs against different species of bacteria (Table 1). The initial concentration of APA_Au NPs was 479.3 μg ml^{-1}. We used the 2-fold dilution method to obtain the MBC of the APA_Au NPs. The value when diluted 32 times was 14.97 and changed to 7.49 with a 64 times dilution. The initial concentration and the serial dilution concentration of N_Au NPs are shown in Table S1.† The antimicrobial properties of N_Au NPs were examined using *E. coli* and *S. aureus* to represent Gram-negative and Gram-positive bacteria, respectively, both sensitive and MDR strains. Au NPs alone or N-heterocyclic molecules alone did not have antibacterial activity at all; however, we found that the N_Au NPs, except APA_Au NPs, were active against Gram-negative and Gram-positive bacteria and their corresponding clinical MDR strains, with the MBC levels being no more than 32 μg ml^{-1}. While the MBC levels of the N-heterocyclic molecules were higher than 128 μg ml^{-1} indicating that the N-heterocyclic molecules alone cannot kill the bacteria at all (Table 1). We speculated that except for that of APA_Au NPs, the surface of the N_Au NPs was positively charged which may facilitate the interaction of these Au NPs with the negatively charged bacteria.

We visualized the morphological change of bacteria treated with N_Au NPs by SEM. In comparison with the control group, most of the NP-treated bacteria merged without an apparent individual cell wall structure, implying the damage of the bacterial structure (Fig. 3). We also used SEM to directly show the morphological change of MDR *E. coli* and MRSA. Compared with the control, most of the N_Au NP-treated bacteria, expect APA_Au NPs for MRSA, merged together and the breakdown of cell structures became increasingly significant, implying the disruption of the bacteria (Fig. S4†).

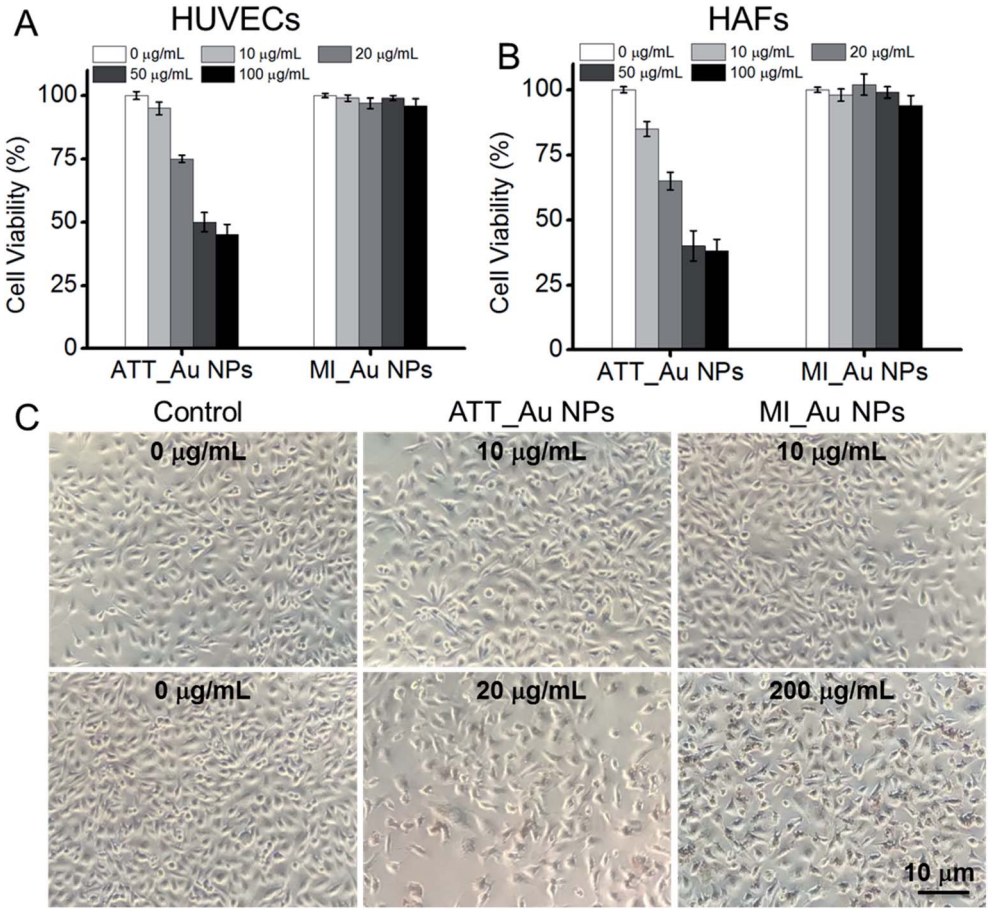

Fig. 7 Biocompatibility of ATT-Au NPs and MI-Au NPs. Concentration-dependent cytotoxicity of ATT_Au NPs and MI_Au NPs cultured with (A) HUVECs and (B) HAFs for 24 h tested with a CCK-8 kit. (C) Morphology of the HUVECs incubated with ATT_Au NPs and MI_Au NPs. The assay without Au NPs was a control.

3.3 Characterization and antibiofilm activity of N_Au NP-coated fabrics

We fabricated N_Au NP-coated fabrics by the sonochemical method. SEM imaging showed that the morphology of the N_Au NP-coated fabrics was uniform (Fig. 4A). Compared with the control group, the protrusions on the surface indicated the successful addition of the N_Au NPs on the fabrics (Fig. 4A). Further, we quantified the amount of gold NPs loaded on the fabrics by ICP. It should be noted that the AMP_Au NPs and MI_Au NPs were better deposited on the surfaces (Fig. 4B).

The antimicrobial properties were examined by first screening the potential of N_Au NP-coated fabrics to compromise the viability of the developed biofilms of *E. coli* and *S. aureus*. All the samples significantly reduced the viability of *S. aureus* while ATT_Au NP- and MI_Au NP-coated fabrics were the most effective with reductions of 2.5 and 5 logs, respectively. AMBT_Au NPs showed comparable effects on *S. aureus* to ATT_Au NPs (Fig. 5). For *E. coli*, the reduction in the biofilm viability was less prominent; nevertheless, MI_Au NP-coated fabrics compromised the biofilm viability by 2 logs (Fig. 5).

AMP_NPs showed comparable effects on *E. coli* to MI_Au NPs. ATT_Au NPs and MI_Au NPs had better antibacterial activities compared with others, due to their higher loading on the surface of the fabrics. Considering these results, we selected ATT_Au NPs and MI_Au NPs as representative NPs for the following experiments, elaborating the examination by adding 3 additional antibiotic-resistant bacterial strains: MRSA, MDR *E. coli*, and MDR *K. pneumoniae*. As shown in Table 2, ATT_Au NPs and MI_Au NPs were far more efficient against Gram-positive bacteria, reducing the viability of *S. aureus* by 2.4 and 5.2 logs, respectively, and of MRSA by 3.5 and 4.1 logs, respectively. Importantly, the developed biofilms of Gram-negative strains used in this study were only slightly affected by ATT_Au NPs (Table 2). However, MI_Au NPs led to significant reductions of 1, 1.3, and 1.9 logs in the biofilm viability of MDR *E. coli*, MDR *K. pneumoniae*, and *E. coli*, respectively (Table 2).

The superiority of MI_Au NPs over ATT_Au NPs was further established using an assay testing the impact of the coated surfaces on the viability of planktonic bacteria (Fig. 6). The antibacterial activity of MI_Au NP-coated fabrics against different bacteria was lower than 10 CFU ml^{-1}, where 10 CFU ml^{-1} was the limit of detection. While ATT_Au NPs partially killed all bacterial strains tested, MI_Au NPs completely eradicated all the bacteria (Fig. 6), due to the higher loading of the MI_Au NPs on the surface of the fabrics. Considering the

comprehensive properties, we chose ATT_Au NP- and MI_Au NP-coated fabrics for the subsequent toxicity experiments, which had better antibacterial activity and antibiofilm activity.

3.4 Biological safety

The biocompatibility of Au NPs is particularly important for further clinical applications. We incubated HUVECs and HAFs with ATT_Au NPs and MI_Au NPs in different concentrations to test the cytotoxicity of the NPs, using the cells cultured without the Au NPs as a control. After 24 h, the cell viability of cells treated with MI_Au NPs remained about 95%, even with a concentration as high as 100 μg ml^{-1}, which means that MI_Au NPs have no toxic effects on mammalian cells and are safe for further *in vivo* characterization (Fig. 7A and B). By contrast, at this high concentration, ATT_Au NPs had significant cytotoxicity (Fig. 7A and B). Nevertheless, ATT_Au NPs showed better biocompatibility than those reported in our previous work,[20] demonstrating that the nanoparticles synthesized under aqueous conditions are safer for mammalian cells than those synthesized in methanol. Furthermore, the HUVEC cells cultured with MI_Au NPs in a high concentration (200 μg ml^{-1}) were either quadrangular or spindle shaped, indicating the good conditions of the cells after incubation with MI_Au NPs for 48 h (Fig. 7C). The cell morphology of HAF cells treated with MI_Au NPs remained slender, even when the concentration was as high as 200 μg ml^{-1}, indicating the good growth condition of the cells and low toxicity of MI_Au NPs (Fig. S3†). All the data demonstrate that MI_Au NPs have a wide range of safe concentrations. We also found that the density of the cells treated with ATT_Au NPs was much lower than that of the control group, while the MI_Au NP group was similar to the control group (Fig. 7C and S3†), which means that the MI_Au NPs could not block the proliferation of the cells. Hence, the MI_Au NPs are highly biocompatible and safer than ATT_Au NPs for potential practical applications.

4 Conclusions

We report a method to prepare fabrics that can prevent the formation of a biofilm by sonochemical decoration with N-heterocyclic molecule-capped Au NPs (N_Au NPs). After screening, MI_Au NPs were proven to have uniform and stable sizes and can be modified on the fiber surface with high loading. Moreover, MI_Au NPs were proven to be an excellent candidate for potential practical applications due to their excellent antibacterial activity and high biosafety. The materials for preparing the antibacterial fabrics are commercially available, low-cost, and stable. The production process is also simple and easy to standardize, which may realize mass-production for clinical applications.

Conflicts of interest

There are no conflicts to declare.

Acknowledgements

We thank the National Natural Science Foundation of China (21761142006, 21535001, 81730051, and 81673039), National Key R&D Program of China (2017YFA0205901, and 2018YFA0902600), the Chinese Academy of Sciences (QYZDJ-SSW-SLH039, 121D11KYSB20170026, and XDA16020902), Shenzhen Bay Laboratory (SZBL2019062801004), Guangdong Innovative and Entrepreneurial Research Team Program (2019ZT08Y191), and Tencent Foundation through the XPLORER PRIZE for the financial support. EB wishes to acknowledge the ISF-NSCF Grant Program (2542/17) for the financial support.

Notes and references

1 D. I. Andersson and D. Hughes, Antibiotic Resistance and Its Cost: Is It Possible to Reverse Resistance?, *Nat. Rev. Microbiol.*, 2010, **8**, 260–271.
2 C. A. Arias and B. E. Murray, Antibiotic-resistant Bugs in the 21st Century – a Clinical Super-challenge, *N. Engl. J. Med.*, 2009, **360**, 439–443.
3 L. Zhang, D. Pornpattananangkul, C. M. J. Hu and C. M. Huang, Development of Nanoparticles for Antimicrobial Drug Delivery, *Curr. Med. Chem.*, 2010, **17**, 585–594.
4 M. J. Hajipour, K. M. Fromm, A. A. Ashkarran, D. J. d. Aberasturi, I. R. d. Larramendi, T. Rojo, V. Serpooshan, W. J. Parak and M. Mahmoudi, Erratum: Antibacterial Properties of Nanoparticles, *Trends Biotechnol.*, 2013, **31**, 61–62.
5 H. Wang, M. Cheng, J. Hu, C. Wang, S. Xu and C. C. Han, Preparation and Optimization of Silver Nanoparticles Embedded Electrospun Membrane for Implant Associated Infections Prevention, *ACS Appl. Mater. Interfaces*, 2013, **5**, 11014–11021.
6 H. Gu, P. L. Ho, E. Tong, L. Wang and B. Xu, Presenting Vancomycin on Nanoparticles to Enhance Antimicrobial Activities, *Nano Lett.*, 2003, **3**, 1261–1263.
7 D. Lee, R. E. Cohen and M. F. Rubner, Antibacterial Properties of Ag Nanoparticle Loaded Multilayers and Formation of Magnetically Directed Antibacterial Microparticles, *Langmuir*, 2005, **21**, 9651–9659.
8 E. de Lucas-Gil, A. Del Campo, L. Pascual, M. Monte-Serrano, J. Menendez, J. F. Fernandez and F. Rubio-Marcos, The Fight against Multidrug-resistant Organisms: The Role of ZnO Crystalline Defects, *Mater. Sci. Eng., C*, 2019, **99**, 575–581.
9 A. P. Nagvenkar, A. Deokar, I. Perelshtein and A. Gedanken, A One-step Sonochemical Synthesis of Stable ZnO–PVA Nanocolloid as a Potential Biocidal Agent, *J. Mater. Chem. B*, 2016, **4**, 2124–2132.
10 Q. U. Naqvi, A. Kanwal, S. Qaseem, M. Naeem, S. R. Ali, M. Shaffique and M. Maqbool, Size-dependent Inhibition of Bacterial Growth by Chemically Engineered Spherical ZnO Nanoparticles, *J. Biol. Phys.*, 2019, **45**, 147–159.
11 R. Chakraborty, R. K. Sarkar, A. K. Chatterjee, U. Manju, A. P. Chattopadhyay and T. Basu, A Simple, Fast and Cost-

effective Method of Synthesis of Cupric Oxide Nanoparticle with Promising Antibacterial Potency: Unraveling the Biological and Chemical Modes of Action, *Biochim. Biophys. Acta*, 2015, **1850**, 845–856.

12 A. Singh, A. Ahmed, K. N. Prasad, S. Khanduja, S. K. Singh, J. K. Srivastava and N. S. Gajbhiye, Antibiofilm and Membrane-Damaging Potential of Cuprous Oxide Nanoparticles against *Staphylococcus aureus* with Reduced Susceptibility to Vancomycin, *Antimicrob. Agents Chemother.*, 2015, **59**, 6882–6890.

13 M. L. Schipper, N. Nakayama-Ratchford, C. R. Davis, N. W. Kam, P. Chu, Z. Liu, X. Sun, H. Dai and S. S. Gambhir, A Pilot Toxicology Study of Single-walled Carbon Nanotubes in a Small Sample of Mice, *Nat. Nanotechnol.*, 2008, **3**, 216–221.

14 H. Ji, H. Sun and X. Qu, Antibacterial Applications of Graphene-based Nanomaterials: Recent Achievements and Challenges, *Adv. Drug Delivery Rev.*, 2016, **105**, 176–189.

15 Y. Liu, L. Shi, L. Su, H. C. van der Mei, P. C. Jutte, Y. Ren and H. J. Busscher, Nanotechnology-based Antimicrobials and Delivery Systems for Biofilm-infection Control, *Chem. Soc. Rev.*, 2019, **48**, 428–446.

16 S. M. Dizaj, F. Lotfipour, M. Barzegar-Jalali, M. H. Zarrintan and K. Adibkia, Antimicrobial Activity of the Metals and Metal Oxide Nanoparticles, *Mater. Sci. Eng., C*, 2014, **44**, 278–284.

17 Y. Zhao, Z. Chen, Y. Chen, J. Xu, J. Li and X. Jiang, Synergy of Non-Antibiotic Drugs and Pyrimidinethiol on Gold Nanoparticles Against Superbugs, *J. Am. Chem. Soc.*, 2013, **135**, 12940–12943.

18 Y. Cui, Y. Zhao, Y. Tian, W. Zhang, X. Lu and X. Jiang, The Molecular Mechanism of Action of Bactericidal Gold Nanoparticles on *Escherichia coli*, *Biomaterials*, 2012, **33**, 2327–2333.

19 X. Yang, J. Yang, L. Wang, B. Ran, Y. Jia, L. Zhang, G. Yang, H. Shao and X. Jiang, Pharmaceutical Intermediate-modified Gold Nanoparticles: against Multidrug-resistant Bacteria and Wound-healing Application via an Electrospun Scaffold, *ACS Nano*, 2017, **11**, 5737–5745.

20 Y. Feng, W. Chen, Y. Jia, Y. Tian, Y. Zhao, F. Long, Y. Rui and X. Jiang, N-Heterocyclic Molecule-capped Gold Nanoparticles as Effective Antibiotics against Multi-drug Resistant Bacteria, *Nanoscale*, 2016, **8**, 13223–13227.

21 J. Bresee, C. M. Bond, R. J. Worthington, C. A. Smith, J. C. Gifford, C. A. Simpson, C. J. Carter, G. Wang, J. Hartman, N. A. Osbaugh, R. K. Shoemaker, C. Melander and D. L. Feldheim, Nanoscale Structure–activity Relationships, Mode of Action, and Biocompatibility of Gold Nanoparticle Antibiotics, *J. Am. Chem. Soc.*, 2014, **136**, 5295–5300.

22 N. Perkas, G. Amirian, S. Dubinsky, S. Gazit and A. Gedanken, Ultrasound-assisted Coating of Nylon 6,6 with Silver Nanoparticles and its Antibacterial Activity, *J. Appl. Polym. Sci.*, 2007, **104**, 1423–1430.

23 M. Soloviev and A. Gedanken, Coating a stainless steel plate with silver nanoparticles by the sonochemical method, *Ultrason. Sonochem.*, 2011, **18**, 356–362.

24 E. Malka, I. Perelshtein, A. Lipovsky, Y. Shalom, L. Naparstek, N. Perkas, T. Patick, R. Lubart, Y. Nitzan, E. Banin and A. Gedanken, Eradication of Multi-Drug Resistant Bacteria by a Novel Zn-doped CuO Nanocomposite, *Small*, 2013, **9**, 4069–4076.

25 I. Perelshtein, G. Applerot, N. Perkas, E. Wehrschetz-Sigl, A. Hasmann, G. M. Guebitz and A. Gedanken, Antibacterial Properties of an In-situ Generated and Simultaneously Deposited Nanocrystalline ZnO on Fabrics, *ACS Appl. Mater. Interfaces*, 2009, **1**, 361–366.

26 I. Perelshtein, G. Applerot, N. Perkas, E. Wehrschuetz-Sigl, A. Hasmann, G. Guebitz and A. Gedanken, CuO–Cotton Nanocomposite: Formation, Morphology, and Antibacterial Activity, *Surf. Coat. Technol.*, 2009, **204**, 54–57.

27 I. Perelshtein, Y. Ruderman, N. Perkas, J. Beddow, G. Singh, M. Vinatoru, E. Joyce, T. J. Mason, M. Blanes, K. Mollá and A. Gedanken, The Sonochemical Coating of Cotton Withstands 65 Washing Cycles at Hospital Washing Standards and Retains its Antibacterial Properties, *Cellulose*, 2013, **20**, 1215–1221.

28 I. Perelshtein, G. Applerot, N. Perkas, J. Grinblat, E. Hulla, E. Wehrschuetz-Sigl, A. Hasmann, G. Guebitz and A. Gedanken, Ultrasound As A "Throwing Stones" Technique for Production of Antibacterial Nanocomposite Textile, *ACS Appl. Mater. Interfaces*, 2010, **2**, 1999–2004.

29 Y. Shai, Mode of Action of Membrane Active Antimicrobial Peptides, *Biopolymers*, 2002, **66**, 236–248.

